Environment International 136 (2020) 105510

Contents lists available at ScienceDirect

Environment International

journal homepage: www.elsevier.com/locate/envint

Toxicity of urban air pollution particulate matter in developing and adult mouse brain: Comparison of total and filter-eluted nanoparticles

Amin Haghani[a], Richard Johnson[a], Nikoo Safi[b], Hongqiao Zhang[a], Max Thorwald[a], Amirhosein Mousavi[c], Nicholas C. Woodward[d], Farimah Shirmohammadi[c], Valerio Coussa[a], John P. Wise Jr[e], Henry Jay Forman[a], Constantinos Sioutas[c], Hooman Allayee[d], Todd E. Morgan[a], Caleb E. Finch[a,f,*]

[a] Leonard Davis School of Gerontology, University of Southern California, Los Angeles, CA, United States
[b] Center for Cancer Prevention and Translational Genomics at the Samuel Oschin Comprehensive Cancer Institute, Cedars-Sinai Medical Center, Los Angeles, CA, United States
[c] Viterbi School of Engineering, University of Southern California, Los Angeles, CA, United States
[d] Department of Preventive Medicine, University of Southern California, Los Angeles, CA, United States
[e] School of Medicine, University of Louisville, Louisville, KY, United States
[f] Dornsife College, University of Southern California, Los Angeles, CA, United States

ARTICLE INFO

Handling Editor: Xavier Querol

Keywords:
PM0.2
Inhaled pollutants
Neurodevelopment
Neuroinflammation

ABSTRACT

Air pollution (AirP) is associated with many neurodevelopmental and neurological disorders in human populations. Rodent models show similar neurotoxic effects of AirP particulate matter (PM) collected by different methods or from various sources. However, controversies continue on the identity of the specific neurotoxic components and mechanisms of neurotoxicity. We collected urban PM by two modes at the same site and time: direct collection as an aqueous slurry (sPM) versus a nano-sized sub-fraction of PM0.2 that was eluted from filters (nPM). The nPM lacks water-insoluble PAHs (polycyclic aromatic hydrocarbons) and is depleted by > 50% in bioactive metals (e.g., copper, iron, nickel), inorganic ions, black carbon, and other organic compounds. Three biological models were used: in vivo exposure of adult male mice to re-aerosolized nPM and sPM for 3 weeks, gestational exposure, and glial cell cultures. In contrast to larger inflammatory responses of sPM in vitro, cerebral cortex responses of mice to sPM and nPM largely overlapped for adult and gestational exposures. Adult brain responses included induction of IFNγ and NF-κB. Gestational exposure to nPM and sPM caused equivalent depressive behaviors. Responses to nPM and sPM diverged for cerebral cortex glutamate receptor mRNA, systemic fat gain and insulin resistance. The shared toxic responses of sPM with nPM may arise from shared transition metals and organics. In contrast, gestational exposure to sPM but not nPM, decreased glutamatergic mRNAs, which may be attributed to PAHs. We discuss potential mechanisms in the overlap between nPM and sPM despite major differences in bulk chemical composition.

1. Introduction

Air pollution (AirP) is associated with adverse impact on human brain functions throughout life, from development, e.g., myelin deficits and risk of autism (Becerra et al., 2013; Peterson et al., 2015), into later ages, e.g., accelerated cognitive decline and risk of dementia (Cacciottolo et al., 2017; Calderon-Garciduenas et al., 2019; Paul et al., 2019; Peters et al., 2019). Rodent models show similar neurotoxic effects of AirP particulate matter (PM). Adult brain responses to various AirP models included inflammatory responses with microglial activation (Liu et al., 2014; Woodward et al., 2018); induction of IFNγ, NF-κB, and TLR4 (Cole et al., 2016; Woodward et al., 2017a); increased amyloidogenesis (Cacciottolo et al., 2017; Levesque et al., 2011); and altered glutamatergic receptors (Morgan et al., 2011). Gestational exposure to AirP activated microglia (Bolton et al., 2012), impaired myelinogenesis (Klocke et al., 2018; Woodward et al., 2017b);

Abbreviations: AirP, air pollution; PM, particulate matter; PAHs, polycyclic aromatic hydrocarbons; nPM, nano-sized particulate matter, filter extraction; sPM, slurry particulate matter; PM0.2, ultrafine particulate matter, diameter < 0.2μm; IPGTTs, i.p. glucose tolerance test; WSOC, water-soluble organic carbon; VACES, versatile aerosol concentration enrichment system

* Corresponding author.
E-mail address: cefinch@usc.edu (C.E. Finch).

https://doi.org/10.1016/j.envint.2020.105510
Received 8 November 2019; Received in revised form 17 January 2020; Accepted 17 January 2020
Available online 28 January 2020

decreased adult neural stem cells (Woodward et al., 2018), and increased depressive behaviors (Davis et al., 2013; Woodward et al., 2018).

Particulate matter (PM) is a heterogeneous mixture that varies widely by time and place in its numerous toxic compounds (e.g., polycyclic aromatic hydrocarbons (PAHs), organic and elemental carbon (OC/EC) and transition metals). However, it is unclear which of these potentially neurotoxic components of AirP are responsible for the injury. While cognitive impairments in several human populations varied in proportion to the ambient density of AirP (Peters et al., 2019), no study to our knowledge has compared the neurotoxicity of AirP from different sources in rodents or cell models. The identification of causative neurotoxic components is challenged by the complexity of the mixtures, the overlapping toxicity of individual components, and their interactions. Our approach to identify some chemical-specific responses in PM mixture is to compare experimental responses of a total PM sample (i.e. collecting all PM components) with a filter-eluted fraction of ultrafine PM that lacks PAHs (Morgan et al., 2011), and is depleted in a wide range of other toxic components (e.g., metals, black carbon, and some organics) (Morgan et al., 2011; Woodward et al., 2017a). Using a high-volume aerosol-into-liquid collector allows the direct collection of ambient PM into aqueous suspension (slurry, sPM) (Wang et al., 2013). The sPM is equivalent in PAH and transition metal composition to ambient PM (Taghvaee et al., 2019).

Toxicological studies of PAHs suggest their importance to the neurotoxicity of AirP in human and rodent models. Epidemiological and clinical studies show correlations of PAH with myelination deficits (Peterson et al., 2015), autistic behavior (Volk et al., 2011), and childhood obesity (Kim et al., 2014). Gestational exposure of rodents to specific PAHs, e.g., benzo(a)pyrene at high dosage, caused adult impairments of the hippocampus, including long-term potentiation, with altered glutamate receptors such as GluN1 (Brown et al., 2007; McCallister et al., 2008; Wormley et al., 2004), oxidative stress and lipid peroxidation in several brain regions (Saunders et al., 2006). Systemic effects include greater post-weaning weight gain, glucose dysregulation, and decreased lipolysis (Irigaray et al., 2009; Irigaray et al., 2006). These toxic effects of gestational PAH exposure resemble those caused by gestational exposure to AirP-PM or diesel exhaust particles (Table S1) (Bolton et al., 2012, 2013; Klocke et al., 2017; Zhang et al., 2018; Zheng et al., 2018). Contrary to expectations, the gestational exposure to nPM, which lacks PAHs, also caused similar long-lasting neurotoxic effects (Davis et al., 2013; Woodward et al., 2019; Woodward et al., 2018). These observations necessitate a direct comparison of nPM with total PM0.2.

2. Methods

2.1. Air pollution sample collection

Ambient nanoscale particulate matter (nPM; particles with aerodynamic diameters less than 0.20 μm) were collected on an 8 × 10 in.-Zeflour PTFE filter (Pall Life Sciences, Ann Arbor, MI) by a High-Volume Ultrafine Particle (HVUP) Sampler (Misra et al., 2002) at 400 L/min flow rate at the Particle Instrumentation Unit of the University of Southern California located within 150 m downwind of a major freeway (I-110). These aerosols represent a mixture of primary emissions ambient PM from vehicular traffic on this freeway. Gravimetric mass (nPM mass concentration) was determined from pre- and post-weighing the filters at 22–24 °C/relative humidity 40–50% by high precision (± 0.001 mg) microbalance (MT5, Mettler Toledo Inc., Columbus, OH). The nPM fraction of filter-deposited PM0.2 was obtained by 30 min aqueous sonication (Morgan et al., 2011). The resuspended nPM mass was quantified as the difference between the total pre-extraction and the post-extraction weight of filters.

The second set of samples (sPM) was collected using the aerosol-into-liquid collector tandem that utilizes the particle-to-droplet growth system via supersaturation of ultrapure water vapor of the versatile aerosol concentration enrichment system (VACES) (Kim et al., 2001a; Kim et al., 2001b). This sampler operates at a flow rate of 200 L/min and collects ambient PM2.5 (i.e, particles with aerodynamic diameters < 2.5 μm) directly as concentrated slurry samples (Wang et al., 2013). Briefly, sampled air is drawn into a saturator tank for mixture with ultrapure water (Milli-Q integral system (Resistivity: 18.2 MΩ•cm, < 1 particulate/mL, Millipore and Sigma-Aldrich, North Carolina, USA) vapor at 30 °C. The particle–vapor mixture then passes through a condensational growth section where it is cooled to about 20 °C; the resulting super-saturation condenses ultrapure water vapor onto incoming particles, which grow to about 3.5–4 mm droplets. Grown droplets are separated from the air stream by inertial impaction and accumulated as concentrated slurry samples. (sPM). Both nPM and sPM samplings were concurrent in May of 2017.

2.2. Characterization of PM components

The re-aerosolized ultrafine nPM and sPM were collected on filters in animal exposure chambers for chemical characterization (Pirhadi et al., 2019). The total elemental composition of the nPM samples was quantified by digestion of a section of the nPM deposited filter using a microwave aided, sealed bomb, mixed acid digestion (nitric acid, hydrofluoric acid, and hydrochloric acid). Digests were subsequently analyzed by high-resolution mass spectrometry (SF-ICPMS) (Herner et al., 2006). Total and Water-Soluble Organic Carbon (TOC/WSOC) analysis was conducted utilizing the Sievers 900 Total Organic Carbon Analyzer (Stone et al., 2009). PAHs were quantified using gas chromatography-mass spectrometry (GC–MS) (Sheesley et al., 2003). The isotopically-labeled internal recovery standards used as spikes include pyrene-D10, benz(a)anthracene-D12, coronene-D12. For PAH assay, AirP filters were extracted by acetone/dichloromethane and derivatized by diazomethane. Black carbon was assayed in re-aerosolized nPM and sPM by an Aethalometer (Model AE51, AethLabs, California, USA). These PM samples were compared to ambient PM0.2 collected on filters from the same site in parallel with the collection of nPM and sPM in 2017. Chemical composition was analyzed by SF-ICPMS and GCMS.

2.3. Animal ethics statement

All animal procedures of this study were approved by the University of Southern California (USC) Institutional Animal Care and Use Committee (IACUC).

2.4. Exposure of adult mice

Young C57BL/6NJ male mice (6–8 weeks; 27.5 ± 2 gm mean weight; n = 10/group) were purchased from Jackson Laboratories. After acclimation for 1 week, mice were exposed to different concentrations of re-aerosolized PM for 45 h over 3 weeks (5 h per day, 3 days per week). Mice were transferred from home cages into sealed exposure chambers that were well ventilated (Morgan et al., 2011). One chamber was the “control” filtered air (FA). Other cages were exposed to three PM levels of approximately 100, 200, and 300 μg/m^3. For 100 and 200 μg/m^3, PM was diluted by filtered air. Mass concentration of re-aerosolized nPM was measured gravimetrically by filters parallel to the exposure stream, before and after exposure. Nebulizer pressure was adjusted to yield similar distributions of particle number size, equivalent to ambient PM0.2 for re-aerosolized nPM and sPM (Fig. S1) (Taghvaee et al., 2019). Thus, sPM for in vivo exposure excluded PM > 0.2 μm.

2.5. Gestational exposure

9-week-old C57BL/6NJ mice were housed as breeding trios (1 male, 2 females) and randomly assigned to each treatment group (nPM, sPM,

FA), 6 breeding trios per group. Mice were exposed to nPM or sPM at 300 μg/m^3 throughout gestation for 5 h/day, 3 days/week for 3 weeks. The five breeding trios per treatment group had viable litters; numbers of offspring were 35 pups (nPM), 30 (sPM), 33 (FA).

2.6. Forced swim

Stress coping strategies were assessed at 11 weeks of age. Mice were placed in a cylindrical water bath at 24–25 °C and recorded for five minutes with latency to the first period of immobility and total time immobile. For glutamatergic functions, at 16 weeks of age, male sPM-exposed mice underwent a second round of forced swim testing 30 min after i.p. MK-801 (0.06 mg/kg) or saline (control).

2.7. Glucose tolerance test

At age 16 weeks, mice underwent i.p. glucose tolerance tests (IPGTTs) (Dinger et al., 2018). After overnight fasting, mice were given i.p glucose (1 mg/g body weight; 10% wt/vol in sterile water). Tail vein blood was sampled at 0, 15, 30, 60, 90, and 120 min post-injection.

2.8. Body weight and composition analyses

Body weight was measured every 1–2 weeks after weaning. Body composition for fat, lean mass, body fluids, and total body water was assessed by NMR (LF90, TD-NMR; Bruker, USA) at 3 ages in weeks 4 to 16.

2.9. Cell fractions

The frontal cerebral cortex (20 mg) was mechanically homogenized in 1x RIPA buffer supplemented with 1 mM Na_3VO_2, 1 mM phenylmethylsulfonyl fluoride (PMSF), 10 mM NaF, phosphatase inhibitor cocktail (Sigma), and Complete Mini EDTA-free Protease Inhibitor Cocktail Tablet (Roche). For biochemical assays, supernatants were obtained by centrifugation 10,000g/10 min. For NF-κB assays, nuclear and cytosolic fractions were obtained from tissue homogenization in sucrose-Tris (STM) buffer with phosphatase and protease inhibitors (Dimauro et al., 2012). After centrifugation (800 g/15 min, 4 °C), the cytosolic supernatant was collected and the nuclear pellet was washed in STM buffer, then resuspended in NET and sonicated. Fraction purity was validated by immunoblotting for nuclear marker histone 3 (H3) and cytosolic glyceraldehyde 3-phosphate dehydrogenase (GAPDH).

2.10. Western blot

Protein lysates (20 μg) were electrophoresed on Criterion 4–15% TGX gels (Biorad) and transferred to PVDF membranes. Following washing with TBS + 0.05% Tween-20 (PBST), membranes were blocked (LiCOR) 1 h at ambient temperature, followed by primary antibody incubation overnight at 4 °C: anti-GluR1 (1:1000, Rabbit polyclonal, Abcam, ab31232), anti-actin (1:5000, mouse, Sigma), anti-NF-κB/p65 (1:750, Rabbit polyclonal, Cell Signaling Technology, D14E12), anti-H3 (1:1000, Rabbit polyclonal, Cell Signaling Technology, D1H2), and anti-GAPDH (1:500, Mouse monoclonal, Santa Cruz Biotechnology, sc-32233). After 1 h incubation with 1:20,000 fluorochrome-conjugated LICOR-antibodies (anti-mouse IRDye 800CW or anti-rabbit IRDye 700CW), blots were scanned and band intensity analyzed by ImageJ.

2.11. Multiplex Immunoassay

Cerebral cortex lysates were analyzed by V-PLEX Proinflammatory Panel 2 immunoassay (Mesoscale Diagnostics, Rockville, MD).

2.12. PCR

Cerebral cortex RNA was extracted by TriZol; cDNA was prepared using qScript cDNA Supermix (Quantabio); gene-specific primers, Table S2. Data were normalized to GAPDH.

2.13. Cell culture

Primary cultures of mixed glia (astrocyte: microglia, 3:1) from rat cerebral cortex of PN day 3–5 were grown in Dulbecco's modified Eagle's medium (DMEM)/F12 (Cellgro, Mediatech, Herndon, VA) containing 10% fetal bovine serum, 1% penicillin/streptomycin and 1% L-glutamine (Woodward et al., 2017a). BV2 microglia (mouse-derived) were similarly cultured. Cytotoxicity of nPM and sPM was assessed by MTT and by CellTiter-Glo Luminescent Cell Viability (Figs. S2–S3).

2.14. Cellular Nitrate/Nitrite production

Conditioned media were assayed for nitric oxide (NO) and NO_2^-/NO_3^- by the Griess reagent (Ignarro et al., 1993).

2.15. NF-κB assay

THP1-Blue™ NF-κB cells (InvivoGen, San Diego, CA) were grown in RPMI 1640 media with 2 mM L-glutamine, 25 mM HEPES, 10% FBS, 100 μg/ml Normocin, and 1% penicillin/streptomycin. THP1-Blue NF-κB cells are derived from human THP1 monocytes by stable transfection of an NF-κB-inducible SEAP reporter (secreted embryonic alkaline phosphatase) (Yang et al., 1997). SEAP1 expression is driven by an interferon-γ promoter fused with five copies of NF-κB consensus response elements. SEAP in media were assessed by enzymatic reaction with QUANTI-Blue™ (InvivoGen).

2.16. Microbial screening

Bacterial growth media for PM samples included BBL Brain Heart Infusion, MacConkey Agar, BD Difco™ LB Broth, and Difco R2A. Samples (100 μl) were incubated at 37 °C/72 h.

2.17. Endotoxin

Levels were assessed by a *Limulus* assay (Pierce LAL chromogenic endotoxin, Thermo Fisher). For LPS neutralization, PM samples were preincubated with Polymyxin B (0, 1, 10 ng/ml) for 20 min/ambient temperature.

2.18. Statistical analysis

Data were analyzed by GraphPad Prism v.7 for ANOVA with multiple test correction. Multivariate modeling was used for cerebral cortex cytokines. Multivariate analysis, heatmaps, Pearson correlations, and univariate linear regression used Rstudio.

3. Results

3.1. Chemical characterization of PM samples

AirP particulate matter (PM) was collected in two modes. The nPM, as used in our prior studies, was collected as nanosized PM0.2 on the filter, and eluted into the water by sonication as an aqueous suspension. The sPM was PM2.5 directly collected from ambient air pollutants into water suspension. Upon re-aerosolization, the size of sPM is fractionated for exposure to PM0.2. Data are shown as analytical results of re-aerosolized (nPM, sPM) to compare with total ambient PM0.2 (Fig. 1).

The chemical composition (per PM mass) of nPM and sPM was equivalent for total organic carbon, whereas nPM had 4-fold less black

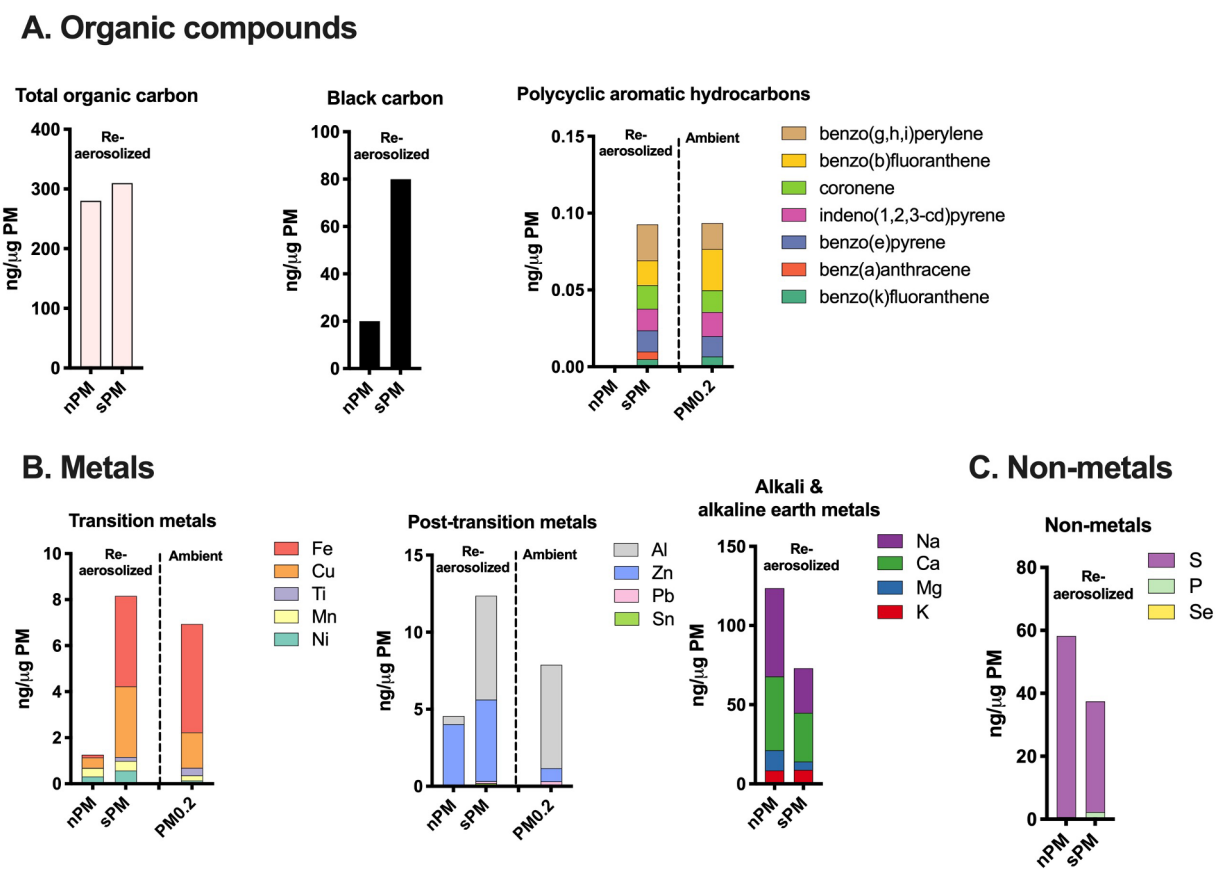

Fig. 1. Chemical composition of re-aerosolized nPM and sPM compared with total ambient air PM0.2 collected in parallel on a filter. (A) Total organic carbon, black carbon, and PAH with concentration > 0.005 ng/μg PM. Indeno(1,2,3-cd)pyrene with 0.015 ng/μg PM concentration and EPA toxicity equivalent factor of 1 was the most toxic PAH species in sPM and ambient PM samples. (B) Metals, transition, and post-transition, alkali and alkaline earth; (C) non-metals. Only elements with > 0.1 ng/μg PM are shown.

carbon and no detectible PAHs (Fig. 1A). The highest PAH levels in sPM were benzo(g,h,i)perylene, benzo(b)fluoranthene, and coronene (0.023, 0.016, and 0.015 ng/μg PM, respectively). Ambient PM0.2 and re-aerosolized sPM had equivalent levels of the major PAHs.

The concentration of iron and other metals was much lower in nPM than sPM (Fig. 1B): iron, 30-fold lower; copper, 6-fold lower; nickel, 2-fold lower; total transition metals, 8-fold lower; post-transition metals, 2-fold lower. nPM had 50% higher levels of other metals and non-metal elements (Fig. 1C) (i.e. Na, Mg, S, Mg). The chemical composition and concentration of nPM agree with prior analyses (Morgan et al., 2011; Woodward et al., 2017a).

An independent sample of nPM and sPM suspensions showed equivalence for levels of organic acids, n-alkanes, hopanes, and steranes, which represent < 0.1% of total organic carbon (Fig. S4).

3.2. Inflammatory responses of cerebral cortex of adult mice to nPM and sPM

Adult mice were exposed for 45 total hours to re-aerosolized nPM and sPM. Both types of PM, with the dose range of 100–300 μg/m^3, induced inflammatory responses in the cerebral cortex, consistent with the responses upon nPM exposure in prior studies (Cheng et al., 2016). Bodyweight was not altered by exposures to nPM or sPM (Fig. S5). Protein levels of IFNγ in the cerebral cortex were induced with similar dose-dependence by nPM and sPM, while nPM caused increased IL1β and decreased IL2 (Fig. 2A). IL6 and TNFα did not respond to nPM or sPM. For mRNA, nPM and sPM decreased TLR4 and MyD88 (Fig. 2B). sPM exposure decreased TLR4 levels more than nPM. GluA1 mRNA was decreased at 300 μg/m^3 by nPM, but not by sPM. GluA1 protein was slightly lowered by nPM (-10%, p = 0.2) (Fig. S6). Nuclear localization of NF-κB/p65 was increased by sPM (Fig. 2C). The cytosolic NF-κB/p65 was increased by nPM. These data suggest that adult exposure to nPM and sPM caused inflammatory responses in the brain, and sPM had a stronger effect.

3.3. Gestational impact of nPM and sPM on behaviors and neuroinflammation in later life

To compare the neurotoxic effects of gestational exposure to nPM and sPM, the dams were exposed to 300 μg/m^3 of nPM or sPM during the three weeks of pregnancy, followed by an examination of their offspring. Compared to controls, the postnatal body weight gains were greater in nPM and sPM by week 4 (juvenile) (Fig. 3A). Body fat was greater only for nPM males by 4 weeks (Fig. 3B). At 16 weeks, glucose tolerance was impaired in nPM males, but not females (Fig. 3C). Changes in glucose tolerance and fat content were correlated (Fig. 3D).

Young adults (age > 10 weeks) after gestational exposure to nPM and sPM showed similar depressive changes (forced swim cognitive test), but the effect was greater on males than females (Fig. 3E). The depression caused by gestational sPM exposure was ameliorated by MK-801, an NMDA glutamate receptor antagonist (Fig. 3F), suggesting altered NMDA pathway may underlie depression caused by gestational exposure. Brains from sPM males were not further analyzed to avoid confounds from MK-801 injection and the second round of forced swim behavior test.

Expression of inflammatory and glutamate associated genes in the cerebral cortex was altered by gestational exposure only in female offspring exposed to sPM (Fig. 3G). Among the examined inflammatory

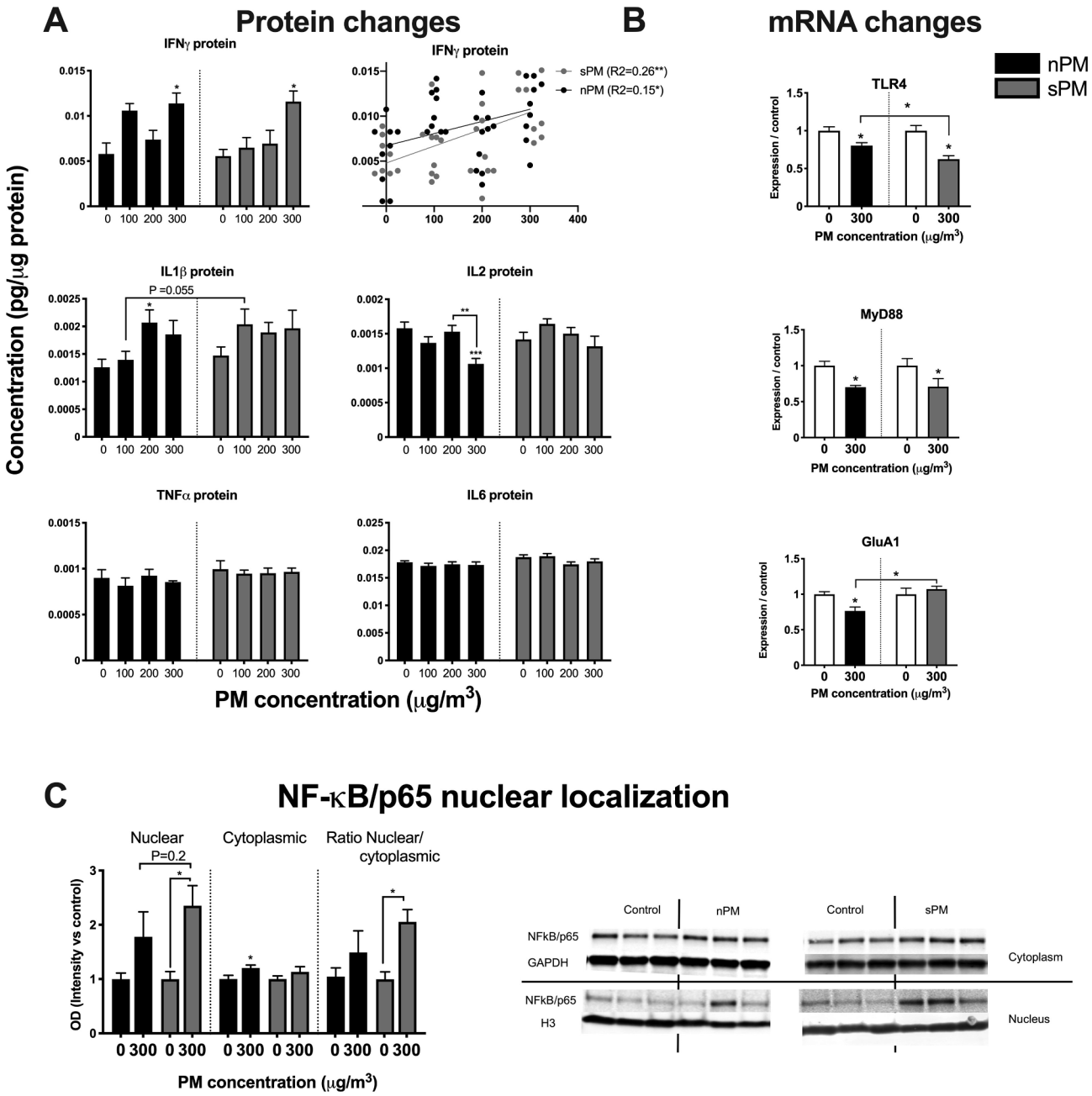

Fig. 2. Cerebral cortex inflammatory responses of nPM and sPM in adult mice. (A) Dose-response of nPM and sPM showed an increase of IFNγ. nPM increased IL1β and decreased IL2. (B) mRNA determination showed decreased TLR4 and MyD88 upon exposure to nPM and sPM. GluA1 was decreased by nPM, but not by sPM. C) NF-κB/p65 nuclear localization. Mean ± SE. Adjusted p-values: < 0.05 (*), < 0.01(**).

mediators, decreased Cox2 (−30%) and iNos (−70%) were the largest responses. The mRNA levels of glutamatergic pathway genes were decreased by 25–35% (Fig. 3G): glutamate receptors (Nmda3a, Nmda2c, GluA1, GluA2, and Glun1), glutamine synthase (Glul), glutaminase (Gls), and glutamate transporters (Glt1, and Glast).

In brief, gestational exposure to nPM and sPM caused depression similarly in later life, but distinct effects were observed, including effects of nPM on metabolism and effects of sPM on glutamate pathways. These effects were sex-dependent.

3.4. *In vitro inflammatory responses of glia cells to nPM and sPM*

To further compare the toxic effects of nPM and sPM, the expression of inflammation-related genes was measured in cultured cells upon exposure. The effects of nPM and sPM on the TLR4 pathway (Fig. 4A), which were activated by AirP in the lung (He et al., 2017) and brain (Woodward et al., 2017a), were examined in two glial cell models. In BV2 microglia, MyD88 and NF-κB1 were equally induced by nPM and sPM, while the expression of TLR4 was not changed (Fig. 4B). The induction of downstream inflammatory mediators, including IL6, IL1β, TNFα, Cox2, and iNOS, was 50% greater by sPM vs nPM (Fig. 4B). These five inflammatory genes shared similar correlations of response to sPM and nPM (heatmap of pairwise Pearson correlations) (Fig. 4C), e.g., IL1β-iNOS and IL1β-Cox2 (Fig. 4D). Nitric oxide (NO) induction was evaluated in mixed glia (Fig. 4E). NO production was induced by an equal scale in response to nPM and sPM (Fig. 4E), similarly, iNOS mRNA was induced 25-fold by both nPM and sPM (Fig. 4F). These data indicate that both nPM and sPM can induce the expression of inflammatory genes, with a stronger effect oft sPM on microglia.

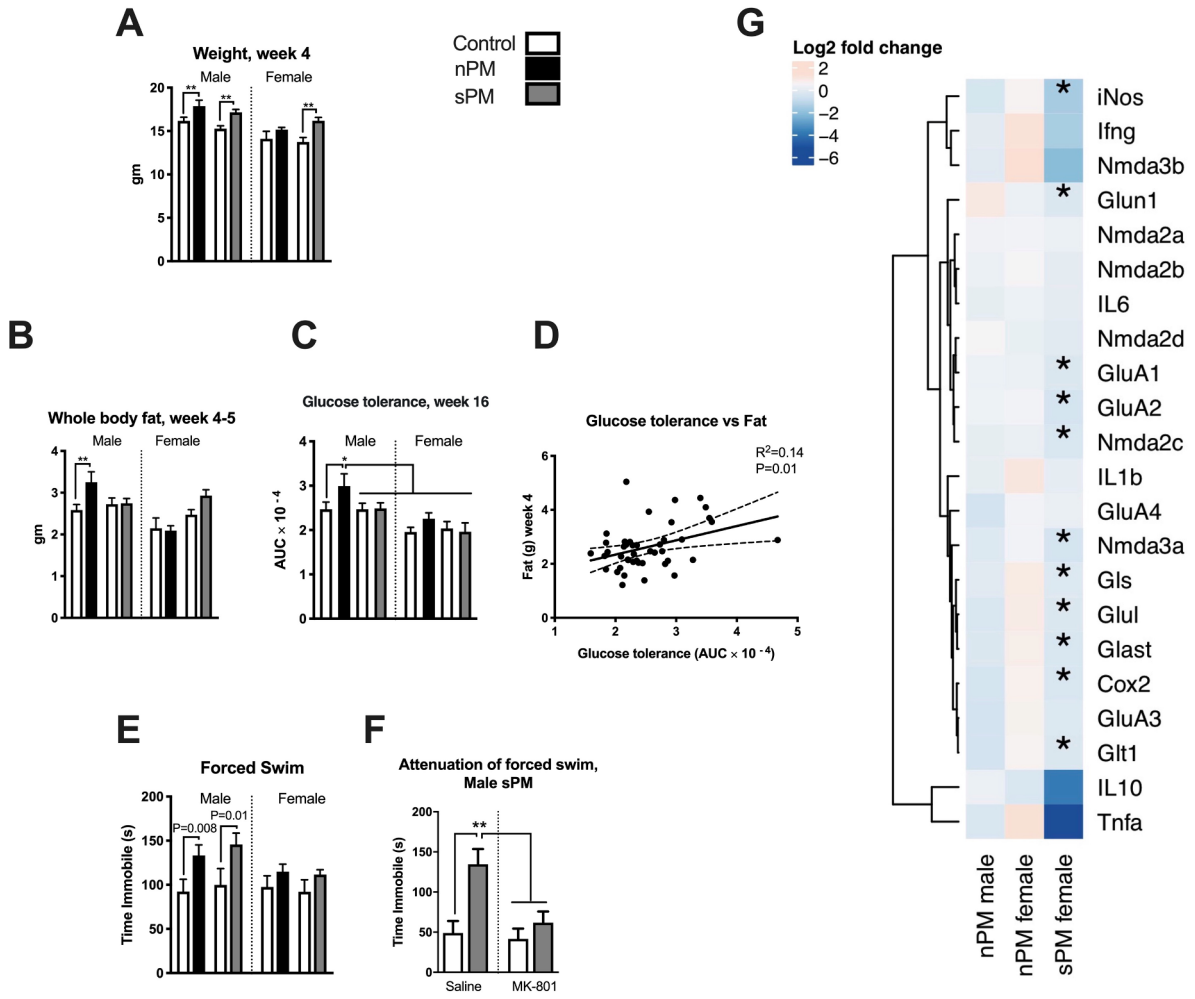

Fig. 3. Effects of gestational exposure to nPM and sPM. (A) Weight difference at age of 4 weeks after gestational exposure to nPM or sPM. (B) Body fat content at the age of 4 weeks, measured by NMR (N = 6–25/group). (C) Glucose tolerance test at the age of 16 weeks after gestational exposure to nPM or sPM (N = 7–13/group). Data are shown as AUC ('area under the curve' for blood glucose changes (mg/dL) during 2 h post glucose challenge). (D) Correlation of glucose tolerance in gestationally nPM exposed offspring at week 16 with body fat content of postnatal week 4. Multiple test correction by Benjamini two-stage Adjusted p-values: < 0.05 (*), < 0.01(**). (E) Depressive behavior of mice assessed by forced swim cognitive test at the age of 11–15 weeks (N = 5–16 mice/group). (F) Attenuation of depression indicator by MK-801 (i.p. 0.06 mg/kg, 30 min before forced swim (N = 5–7/group). G) RT-qPCR analysis of the selected glutamatergic and inflammatory genes in the cerebral cortex (N = 7–17/group). Heatmap represents log2 fold changes of mRNA relative to non-exposed controls of each group. * significance at 5% FDR rate, exposed vs control.

3.5. In vitro NF-κB induction by nPM and sPM

The time- and dose-dependent response of NF-κB activity to nPM and sPM was studied with a human monocyte reporter for NF-κB (Fig. 5A–B). At 5 μg/ml, sPM had 50% steeper dose-response slope than nPM (Fig. 5B), paralleling BV2 cell responses; at 1 μg/ml, neither nPM nor sPM activated NF-κB. The stronger NF-κB activation by sPM matches the greater mRNA induction of 5 genes regulated by NF-κB in BV2 cells (Fig. 4B).

Because sPM and nPM are collected from ambient air, we investigated their microbial content. On four growth media (Brain Heart infusion, MacConkey, LB, R2A), the sPM samples had at least 10-fold greater microbial growth with more species than nPM (Table S3).

In vitro cell cultures included antibiotics to minimize bacterial growth, for up to 24 h incubation with sPM or nPM, cell culture medium did not manifest turbidity and no bacterial contamination was observed (data not shown). Endotoxin (LPS), a trigger of inflammatory responses, was also assayed. Both nPM and sPM had 0.014 EU/μg PM of LPS (Fig. 5C), or approximately 1.4 pg LPS/μg PM (1.4×10^{-4} pmol LPS/μg PM) (Reich et al., 2018). Neutralization of LPS activity by polymyxin B attenuated 40% of the nPM mediated NF-κB response (Fig. 5D). In contrast, NF-κB activation by sPM was not altered by polymyxin B with a concentration of up to 10 ng/ml.

4. Discussion

Despite the compositional differences of nPM and sPM, they shared neurotoxic and systemic effects for adult and gestational exposure, and cell model responses (Fig. 6). In contrast with sPM, nPM lacked detectable PAHs; the metal content of nPM was lower, differing more for the transition than non-transition metals, discussed below. Moreover, sPM had at least a 10-fold higher microbial load than nPM. Thus, the shared neurotoxicity of nPM and sPM may be attributed to transition metals and unidentified organic carbon compounds among many other components. In contrast, gestational exposure to sPM but not nPM, decreased glutamatergic mRNAs, which may be attributed to PAHs. Below, we discuss potential mechanisms underlying shared neurotoxic responses of nPM and sPM. We also discuss the distinct responses that could be attributed to compositional differences of nPM and sPM. Additionally, several PM characteristics such as surface chemistry and reactivity that are currently missing in the experimental neuroscience framework could play a predominant role in AirP neurotoxicity.

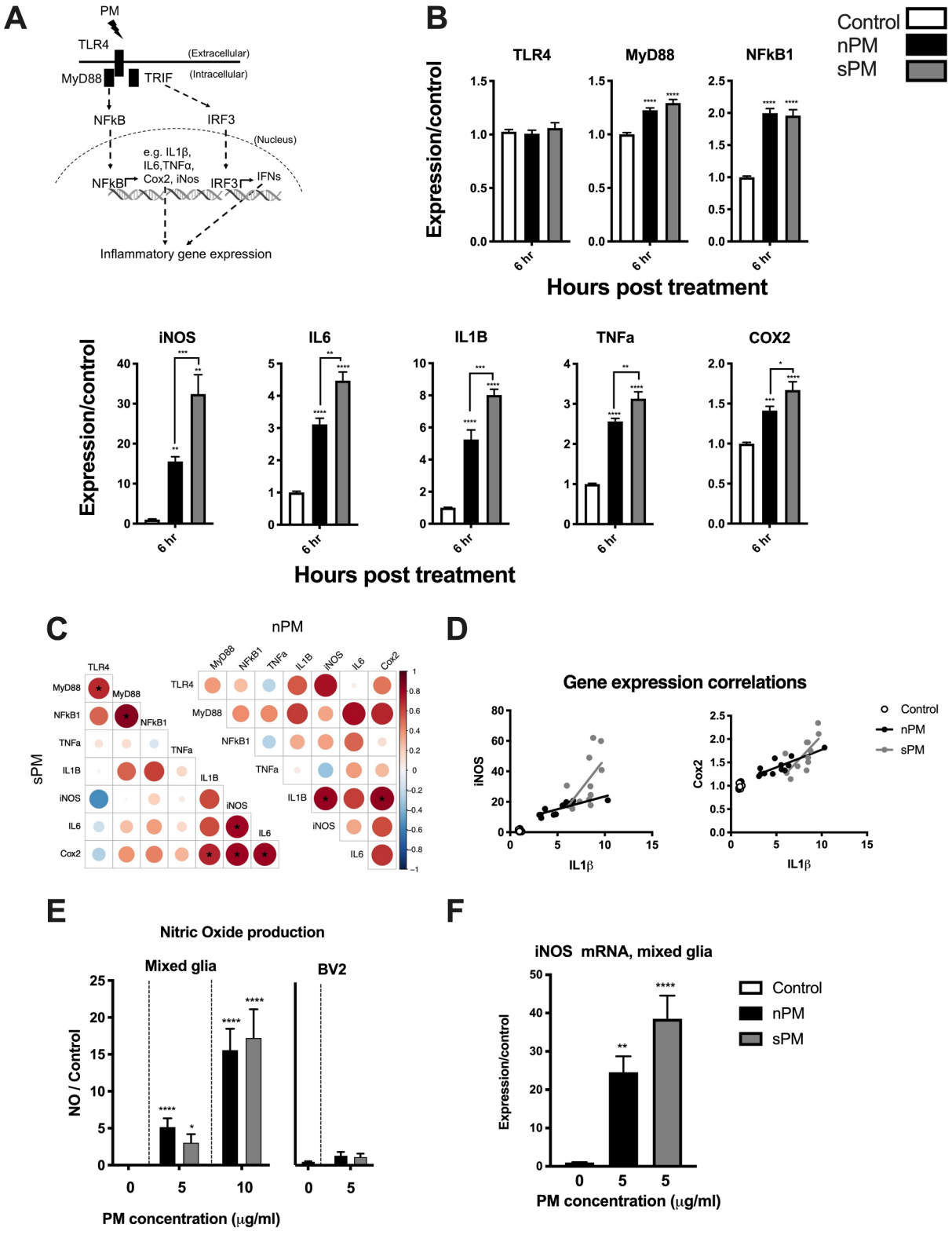

Fig. 4. In vitro inflammatory gene responses to nPM and sPM in glia. (A) Schema of PM mediated TLR4 pathway activation and inflammatory gene responses. (B) mRNA levels of downstream inflammatory genes after 6 hr exposure to 5 μg/ml nPM or sPM in BV2 microglial cells (RT-qPCR; N = 6/group × 2). (C) Heatmap of pairwise Pearson correlations of mRNA response. (D) IL1β-iNOS and IL1β-Cox2 as examples of inflammatory genes with positively correlated response to nPM and sPM. (E) Dose-response of nitric oxide (NO) production after 24 h of exposure to nPM and sPM; Greiss assay (N = 6–8/group, an average of 3 independent replicates). (F) Induction of iNOS mRNA (RT-qPCR) by 5 μg/ml nPM and sPM in mixed glia (N = 6/group, duplicate average). Mean ± SE. Adjusted P-values: < 0.05(*), < 0.01(**), < 0.001(***), < 0.0001(****), compared with vehicle control.

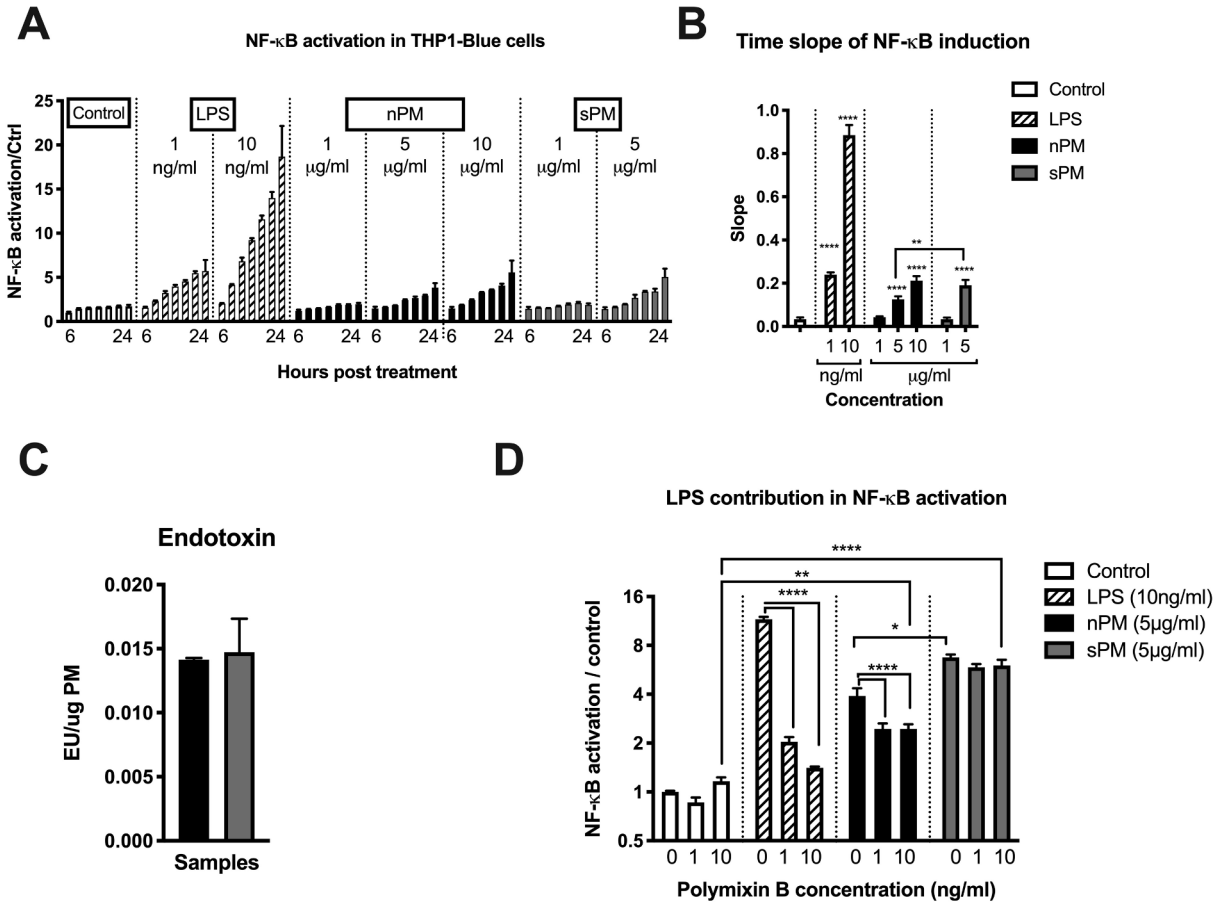

Fig. 5. NF-κB response to nPM and sPM in THP1-blue monocytes. (A) Dose- and time response of NF-κB induction by nPM, sPM, and LPS at 3-h intervals during 6–24 h exposure. (B) Slopes of NF-κB responses during 24 h of exposure to nPM, sPM, and LPS calculated by linear regression (N = 4/group). (C) Endotoxin levels in nPM and sPM, measured by *Limulus* amoebocyte lysate assay (LAL). EU ~ 100 pg LPS (10,000 g/mol) (Hochstein et al. 1983; Reich et al. 2018). D) Contribution of LPS to NF-κB responses of THP1-blue monocytes. LPS contributed up to 40% of NF-κB response in nPM and not sPM. Mean ± SE. Adjusted P-values: < 0.05 (*), < 0.01(**), < 0.001(***), < 0.0001(****), compared with vehicle control.

Shared responses to nPM and sPM were observed in all three models. Three-week exposure of adult mice to nPM or sPM (45 h total) induced a dose-dependent increase of IFNγ, IL1β, and activated the TLR4-NFκB pathway in the cerebral cortex. Also, gestational exposure of nPM and sPM caused similar depressive behaviors in adult mice with sex specificity for males, which extends prior findings by us (Davis et al., 2013; Woodward et al., 2018) and others (Bolton et al., 2012; Klocke et al., 2018). In cell models, both nPM and sPM samples induced

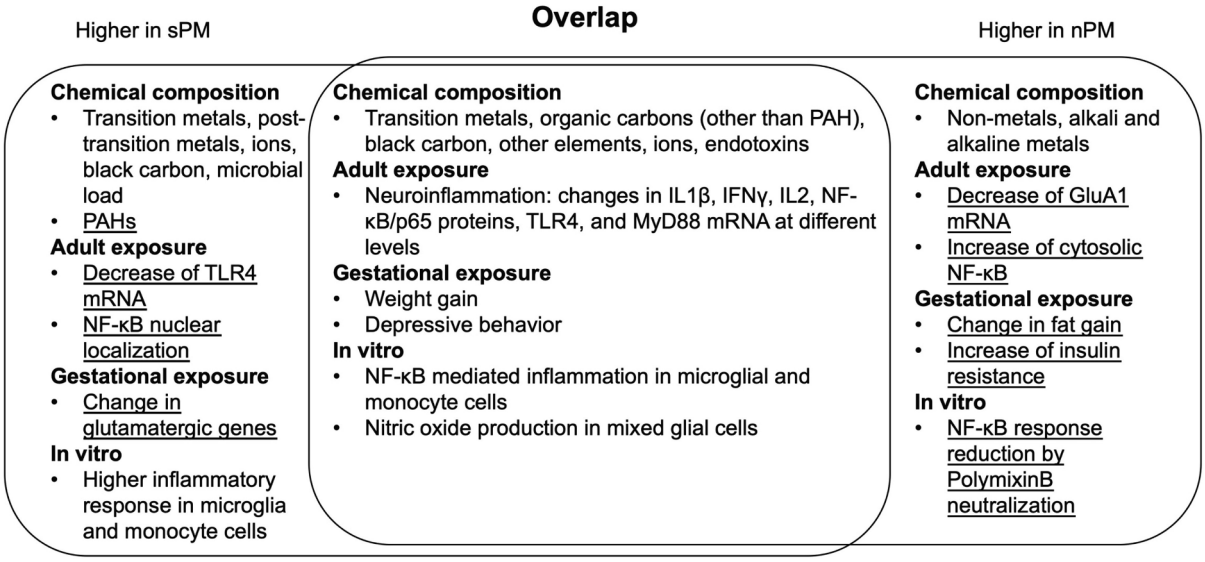

Fig. 6. Summary of the chemical composition and biological effects of nPM and sPM. Underline indicates distinct effects or chemical components of nPM and sPM.

NF-κB mediated inflammation and nitric oxide production. These results suggest that the components and particle characteristics of nPM sufficed to cause neurotoxicity in the 3-week gestational and adult exposures, and in cell models. We provisionally conclude that PAHs, which are absent from nPM, have a minor contribution to neuroinflammation for the 3-week duration of exposure.

Metal content was consistently lower in nPM than sPM: two transition metals differed greatly (Cu, 6-fold; iron, 30-fold), while Ni, Mn, and Zn were within 50%. As noted for PAH, responses to sPM and nPM were shared extensively. Nickel may be a shared neurotoxicant. In a mouse model, inhalation exposure to 1 mg/m^3 nickel nanoparticles caused a rapid doubling of brain Ab40 and 42 (this high level is within OSHA limits) (Kim et al., 2012). However, the content of iron, nickel, or other metals in nPM and sPM did not correlate with the induction of NF-κB, nitric oxide, or lipid membrane oxidation in cell-based assays, or in the brain with microglial activation, proinflammatory cytokines, or Aβ42 (Zhang et al., 2019).

Besides the total metal content, we must also consider the distribution of particle surfaces which contact cells and fluids. The surface chemistry of the particles can largely determine the adsorption of opsonizing proteins such as phospholipids and acute phase proteins in broncho-alveolar lavage fluids (Kendall et al., 2004). Surface chemistry also alters PM distribution in different organs, biotransformation, and clearance of the particles (Stepien et al., 2018). Non-organic PM0.2 varies widely in surface reactivity, e.g., SiO_2 (quartz) and black carbon, assayed as inflammatory cell responses in the lungs (Duffin et al., 2007; Lison et al., 1997). The bioactivity of metals depends upon their surface availability, rather than the total content per particle, which is not equivalent to their molarity in solution. For example, NF-κB induction in THP1 monocytes was dependent on the surface iron of natural silica particles, while equal amounts of iron in solution failed to activate NF-κB (Premasekharan et al., 2011). This might explain the broad similarity of nPM and sPM activity despite having 5-fold less transition metals. Iron and other metals on particle surfaces, while a minute fraction of the total, could contribute to the in vivo neurotoxicity of nPM if it is upon the surface of particles.

The toxicity of PM is sensitive to aerosol acidity and consequently metal solubility (Fang et al., 2017). For example, the sulfate content of the PM can produce acidic aerosols, dissolve primary transition metals, and increase the oxidative potential of PM (Fang et al., 2017). Future studies should consider the acidity of nPM, sPM, and other PM samples collected at different sites or by different methods.

Our study presents the first direct neurotoxic comparison of two kinds of ambient PM with large compositional differences. While the responses of nPM and sPM largely overlapped, there were some differences. sPM caused higher NF-κB response in glial and THP1 cells, induced nuclear localization of NF-κB/P65, and higher downregulation of TLR4 mRNA in the cerebral cortex of adult animals. Larger sPM response was stronger in vitro, which may be attributed to direct physical exposure to PM at shorted duration. Glutamatergic effects of PM after an adult or gestational exposure differed between nPM and sPM: GluA1 mRNA was only decreased in nPM exposed adults; several glutamatergic genes were only downregulated in animals gestationally exposed to sPM. Fat gain and also an increase of glucose tolerance were unique to males that were prenatally exposed to nPM.

The present data do not allow identification of the chemical classes underlying the different responses to nPM and sPM. While nPM samples are depleted in PAHs and several transition metals, they are enriched in non-metals, alkali and alkaline earth metals (Fig. 1B-C). The unique responses of nPM can be due to lack of PAHs, or enrichment of specific classes of other chemicals. For example, depending on the route of the exposure, endpoint, and dosage, PAHs can be potent immune/inflammation activators or suppressors (Abdel-Shafy and Mansour, 2016; Blanton et al., 1986; Burchiel and Luster, 2001; Dean et al., 1986; Ward et al., 1984). Thus, depletion in PAHs could increase the inflammatory responses of nPM that lead to a higher fat gain and increase of glucose tolerance. On the other hand, gestational exposure to specific PAHs, e.g., benzo(a)pyrene at high dose altered hippocampal glutamatergic function and receptors such as Glun1 (Brown et al., 2007; McCallister et al., 2008; Wormley et al., 2004). A similar decrease of Glun1 from gestational exposure to sPM might indicate PAH contribution.

Because endotoxins induce inflammatory responses, we titrated endotoxin activity with polymyxin B, a polycationic antibiotic that binds to diverse bacterial lipopolysaccharides. Polymyxin B attenuated NF-κB induction in THP-1 monocytes for nPM but did not alter sPM activity. This suggests that nPM and sPM have different endotoxin compositions, which is consistent with the greater density and diversity of viable bacteria in sPM than nPM on four growth media. The binding stoichiometry of polymyxin differs widely between LPS chemotypes by length and chemistry of sugar chains on the bacterial outer walls (Brandenburg et al., 2005). Gram-negative bacteria have an additional target of polymyxin B in their secreted outer membrane vesicles which enhance LPS inflammatory activity (Pfalzgraff et al., 2019). Because the THP-1 cell assay includes antibiotics, the greater inflammatory activity of sPM in vitro could represent its higher levels of iron and other transition metals, and potential interactions with endotoxins.

AirP neurotoxicity may be mediated by the direct impact of particles that reach the brain by inhalation or ingestion, and indirectly by systemic responses. Thus, we do not know the pathways leading to elevated brain levels of copper, iron-rich magnetite, and zinc in highly polluted cities (Calderon-Garciduenas et al., 2013; Maher et al., 2016). While some PM may be transported directly into the brain by olfactory neurons (Forman and Finch 2018; Ibanez et al., 2019; Oberdorster et al., 2005), the bulk of inhaled particles and gases are received by the lung (Li et al., 2016). The 'lung-to-brain' path may include some direct transfer of PM to the brain by the circulation, but also includes systemic inflammatory responses (Aragon et al., 2017; Mumaw et al., 2016). A systemic effect of AirP on the developing brain seems likely because most PM is trapped by maternal lungs and placenta (Ho et al., 2017). Other systemic effects are due to inhalation of nitrogen dioxide (NO_2), ozone (O_3), and sulfur dioxide (SO_2), which are rapidly quenched in contact with respiratory tract fluids yet cause neurotoxicity in the brain. Some of these responses include brain glutamatergic responses (e.g., decrease of hippocampal GluA1, GluA2, and Grin2a proteins) and activated MAPK signaling by NO2 (Yan et al., 2016), decrease of mitochondrial activity in cerebellum and increase of Aβ by O3 (Tyler et al., 2018; Valdez et al., 2019), and a dose-response increase of iNOS, Cox2, and ICAM1 proteins in the brain by SO2 (Sang et al., 2010). Thus, the indirect effects of lung-to-brain by circulatory factors may underlie the similar neurotoxicity of exposure to gases and PM (Mumaw et al., 2016).

In sum, the current study demonstrated that nPM neurotoxicity highly overlapped with sPM during short term exposure in adulthood or development. A critical unknown is the amount of inhaled PM and its subcomponents that reaches the brain, PM surface chemistry, and particle structure, which may vary widely by PM sources. Further analysis might consider the use of synthetic nanoparticles containing characterized surface components and longer exposure times.

Acknowledgment

We thank Dr. Steven E. Finkel and Dr. Christopher H. Corzett (Dornsife College, USC) for providing the bacterial growth media and advising on the microbial screen.

Author contribution

Design research: A.H., T.E.M., C.E.F., N.S.; Performed research: Adult exposure, A.H., N.S.; Gestational exposure, R.J., N.W., N.S., A.H. Methodology, A.H., R.J., N.S., H.J.Z., M.T., N.W., V.C.; nPM collection and characterization, A.H.M., F.S., C.S. J.W. Jr. Analyzed data: A.H. Writing: A.H., C.E.F., T.E.M, R.J., M.T., H.J.Z., H.F. Supervision: Project Administration, and Funding Acquisition: C.E.F.

Funding

We are grateful for support by the National Institute of Aging (NIA) of United States: Caleb E Finch (R01-AG051521, P50-AG05142, P01-AG055367), Amin Haghani (T32-AG052374, Kelvin J.A. Davis), Max Thorwald (T32-AG000037, Eileen M Crimmins); and the National Institute of Environmental Health Sciences (NIEHS) of United States: Henry Jay Forman (ES023864).

Declaration of Competing Interest

The authors have no conflicts of interest to declare.

Appendix A. Supplementary material

Supplementary data to this article can be found online at https://doi.org/10.1016/j.envint.2020.105510.

References

Abdel-Shafy, H.I., Mansour, M.S.M., 2016. A review on polycyclic aromatic hydrocarbons: source, environmental impact, effect on human health and remediation. Egypt. J. Petrol. 25, 107–123. https://doi.org/10.1016/j.ejpe.2015.03.011.

Aragon, M.J., Topper, L., Tyler, C.R., Sanchez, B., Zychowski, K., Young, T., Herbert, G., Hall, P., Erdely, A., Eye, T., Bishop, L., Saunders, S.A., Muldoon, P.P., Ottens, A.K., Campen, M.J., 2017. Serum-borne bioactivity caused by pulmonary multiwalled carbon nanotubes induces neuroinflammation via blood-brain barrier impairment. Proc. Natl. Acad. Sci. USA 114, E1968–E1976. https://doi.org/10.1073/pnas.1616070114.

Becerra, T.A., Wilhelm, M., Olsen, J., Cockburn, M., Ritz, B., 2013. Ambient air pollution and autism in Los Angeles county, California. Environ. Health Perspect. 121, 380–386. https://doi.org/10.1289/ehp.1205827.

Blanton, R.H., Lyte, M., Myers, M.J., Bick, P.H., 1986. Immunomodulation by polyaromatic hydrocarbons in mice and murine cells. Cancer Res. 46, 2735–2739.

Bolton, J.L., Huff, N.C., Smith, S.H., Mason, S.N., Foster, W.M., Auten, R.L., Bilbo, S.D., 2013. Maternal stress and effects of prenatal air pollution on offspring mental health outcomes in mice. Environ. Health. Perspect. 121, 1075–1082. https://doi.org/10.1289/ehp.1306560.

Bolton, J.L., Smith, S.H., Huff, N.C., Gilmour, M.I., Foster, W.M., Auten, R.L., Bilbo, S.D., 2012. Prenatal air pollution exposure induces neuroinflammation and predisposes offspring to weight gain in adulthood in a sex-specific manner. FASEB. J. 26, 4743–4754. https://doi.org/10.1096/fj.12-210989.

Brandenburg, K., David, A., Howe, J., Koch, M.H., Andra, J., Garidel, P., 2005. Temperature dependence of the binding of endotoxins to the polycationic peptides polymyxin B and its nonapeptide. Biophys. J. 88, 1845–1858. https://doi.org/10.1529/biophysj.104.047944.

Brown, L.A., Khousbouei, H., Goodwin, J.S., Irvin-Wilson, C.V., Ramesh, A., Sheng, L., McCallister, M.M., Jiang, G.C., Aschner, M., Hood, D.B., 2007. Down-regulation of early ionotrophic glutamate receptor subunit developmental expression as a mechanism for observed plasticity deficits following gestational exposure to benzo(a) pyrene. Neurotoxicology 28, 965–978. https://doi.org/10.1016/j.neuro.2007.05.005.

Burchiel, S.W., Luster, M.I., 2001. Signaling by environmental polycyclic aromatic hydrocarbons in human lymphocytes. Clin. Immunol. 98, 2–10. https://doi.org/10.1006/clim.2000.4934.

Cacciottolo, M., Wang, X., Driscoll, I., Woodward, N., Saffari, A., Reyes, J., Serre, M.L., Vizuete, W., Sioutas, C., Morgan, T.E., Gatz, M., Chui, H.C., Shumaker, S.A., Resnick, S.M., Espeland, M.A., Finch, C.E., Chen, J.C., 2017. Particulate air pollutants, APOE alleles and their contributions to cognitive impairment in older women and to amyloidogenesis in experimental models. Transl. Psychiatry 7, e1022. https://doi.org/10.1038/tp.2016.280.

Calderon-Garciduenas, L., Reynoso-Robles, R., Gonzalez-Maciel, A., 2019. Combustion and friction-derived nanoparticles and industrial-sourced nanoparticles: The culprit of Alzheimer and Parkinson's diseases. Environ. Res. 176, 108574. https://doi.org/10.1016/j.envres.2019.108574.

Calderon-Garciduenas, L., Serrano-Sierra, A., Torres-Jardon, R., Zhu, H., Yuan, Y., Smith, D., Delgado-Chavez, R., Cross, J.V., Medina-Cortina, H., Kavanaugh, M., Guilarte, T.R., 2013. The impact of environmental metals in young urbanites' brains. Exp. Toxicol. Pathol. 65, 503–511. https://doi.org/10.1016/j.etp.2012.02.006.

Cheng, H., Saffari, A., Sioutas, C., Forman, H.J., Morgan, T.E., Finch, C.E., 2016. Nanoscale particulate matter from urban traffic rapidly induces oxidative stress and inflammation in olfactory epithelium with concomitant effects on brain. Environ. Health. Perspect. 124, 1537–1546. https://doi.org/10.1289/EHP134.

Cole, T.B., Coburn, J., Dao, K., Roque, P., Chang, Y.C., Kalia, V., Guilarte, T.R., Dziedzic, J., Costa, L.G., 2016. Sex and genetic differences in the effects of acute diesel exhaust exposure on inflammation and oxidative stress in mouse brain. Toxicology 374, 1–9. https://doi.org/10.1016/j.tox.2016.11.010.

Davis, D.A., Bortolato, M., Godar, S.C., Sander, T.K., Iwata, N., Pakbin, P., Shih, J.C., Berhane, K., McConnell, R., Sioutas, C., Finch, C.E., Morgan, T.E., 2013. Prenatal exposure to urban air nanoparticles in mice causes altered neuronal differentiation and depression-like responses. PLoS One 8, e64128. https://doi.org/10.1371/journal.pone.0064128.

Dean, J.H., Ward, E.C., Murray, M.J., Lauer, L.D., House, R.V., Stillman, W., Hamilton, T.A., Adams, D.O., 1986. Immunosuppression following 7,12-dimethylbenz[a]anthracene exposure in B6C3F1 mice–II. Altered cell-mediated immunity and tumor resistance. Int. J. Immunopharmacol. 8, 189–198. https://doi.org/10.1016/0192-0561(86)90058-5.

Dimauro, I., Pearson, T., Caporossi, D., Jackson, M.J., 2012. A simple protocol for the subcellular fractionation of skeletal muscle cells and tissue. BMC. Res. Notes 5, 513. https://doi.org/10.1186/1756-0500-5-513.

Dinger, K., Mohr, J., Vohlen, C., Hirani, D., Hucklenbruch-Rother, E., Ensenauer, R., Dotsch, J., Alejandre Alcazar, M.A., 2018. Intraperitoneal glucose tolerance test, measurement of lung function, and fixation of the lung to study the impact of obesity and impaired metabolism on pulmonary outcomes. J. Vis. Exp. https://doi.org/10.3791/56685.

Duffin, R., Tran, L., Brown, D., Stone, V., Donaldson, K., 2007. Proinflammogenic effects of low-toxicity and metal nanoparticles in vivo and in vitro: highlighting the role of particle surface area and surface reactivity. Inhal. Toxicol. 19, 849–856. https://doi.org/10.1080/08958370701479323.

Fang, T., Guo, H., Zeng, L., Verma, V., Nenes, A., Weber, R.J., 2017. Highly acidic ambient particles, soluble metals, and oxidative potential: a link between sulfate and aerosol toxicity. Environ. Sci. Technol. 51, 2611–2620. https://doi.org/10.1021/acs.est.6b06151.

Forman, H.J., Finch, C.E., 2018. A critical review of assays for hazardous components of air pollution. Free. Radic. Biol. Med. 117, 202–217. https://doi.org/10.1016/j.freeradbiomed.2018.01.030.

He, M., Ichinose, T., Yoshida, Y., Arashidani, K., Yoshida, S., Takano, H., Sun, G., Shibamoto, T., 2017. Urban PM2.5 exacerbates allergic inflammation in the murine lung via a TLR2/TLR4/MyD88-signaling pathway. Sci. Rep. 7, 11027. https://doi.org/10.1038/s41598-017-11471-y.

Herner, J.D., Green, P.G., Kleeman, M.J., 2006. Measuring the trace elemental composition of size-resolved airborne particles. Environ. Sci. Technol. 40, 1925–1933. https://doi.org/10.1021/es052315q.

Ho, D., Leong, J.W., Crew, R.C., Norret, M., House, M.J., Mark, P.J., Waddell, B.J., Iyer, K.S., Keelan, J.A., 2017. Maternal-placental-fetal biodistribution of multimodal polymeric nanoparticles in a pregnant rat model in mid and late gestation. Sci. Rep. 7, 2866. https://doi.org/10.1038/s41598-017-03128-7.

Hochstein, H.D., Mills, D.F., Outschoorn, A.S., Rastogi, S.C., 1983. The processing and collaborative assay of a reference endotoxin. J. Biol. Stand. 11, 251–260. https://doi.org/10.1016/S0092-1157(83)80013-4.

Ibanez, C., Suhard, D., Elie, C., Ebrahimian, T., Lestaevel, P., Roynette, A., Dhieux-Lestaevel, B., Gensdarmes, F., Tack, K., Tessier, C., 2019. Evaluation of the Nose-to-brain transport of different physicochemical forms of uranium after exposure via inhalation of a UO4 aerosol in the rat. Environ. Health. Perspect. 127, 97010. https://doi.org/10.1289/EHP4927.

Ignarro, L.J., Fukuto, J.M., Griscavage, J.M., Rogers, N.E., Byrns, R.E., 1993. Oxidation of nitric oxide in aqueous solution to nitrite but not nitrate: comparison with enzymatically formed nitric oxide from L-arginine. Proc. Natl. Acad. Sci. USA 90, 8103–8107. https://doi.org/10.1073/pnas.90.17.8103.

Irigaray, P., Lacomme, S., Mejean, L., Belpomme, D., 2009. Ex vivo study of incorporation into adipocytes and lipolysis-inhibition effect of polycyclic aromatic hydrocarbons. Toxicol. Lett. 187, 35–39. https://doi.org/10.1016/j.toxlet.2009.01.021.

Irigaray, P., Ogier, V., Jacquenet, S., Notet, V., Sibille, P., Mejean, L., Bihain, B.E., Yen, F.T., 2006. Benzo[a]pyrene impairs beta-adrenergic stimulation of adipose tissue lipolysis and causes weight gain in mice. A novel molecular mechanism of toxicity for a common food pollutant. FEBS. J. 273, 1362–1372. https://doi.org/10.1111/j.1742-4658.2006.05159.x.

Kendall, M., Guntern, J., Lockyer, N.P., Jones, F.H., Hutton, B.M., Lippmann, M., Tetley, T.D., 2004. Urban PM2.5 surface chemistry and interactions with bronchoalveolar lavage fluid. Inhal. Toxicol. 16 (Suppl 1), 115–129. https://doi.org/10.1080/08958370490443204.

Kim, H.W., Kam, S., Lee, D.H., 2014. Synergistic interaction between polycyclic aromatic hydrocarbons and environmental tobacco smoke on the risk of obesity in children and adolescents: The U.S. National Health and Nutrition Examination Survey 2003–2008. Environ. Res. 135, 354–360. https://doi.org/10.1016/j.envres.2014.08.032.

Kim, S., Jaques, P.A., Chang, M.C., Barone, T., Xiong, C., Friedlander, S.K., Sioutas, C., 2001a. Versatile aerosol concentration enrichment system (VACES) for simultaneous in vivo and in vitro evaluation of toxic effects of ultrafine, fine and coarse ambient particles - Part II: Field evaluation. J. Aerosol. Sci. 32, 1299–1314. https://doi.org/10.1016/S0021-8502(01)00058-1.

Kim, S., Jaques, P.A., Chang, M.C., Froines, J.R., Sioutas, C., 2001b. Versatile aerosol concentration enrichment system (VACES) for simultaneous in vivo and in vitro evaluation of toxic effects of ultrafine, fine and coarse ambient particles - Part I: Development and laboratory characterization. J. Aerosol. Sci. 32, 1281–1297. https://doi.org/10.1016/S0021-8502(01)00057-X.

Kim, S.H.; Knight, E.M.; Saunders, E.L.; Cuevas, A.K.; Popovech, M.; Chen, L.C.; Gandy, S. Rapid doubling of Alzheimer's amyloid-beta40 and 42 levels in brains of mice exposed to a nickel nanoparticle model of air pollution. F1000Res 2012;1:70, doi:http://doi.org/10.12688/f1000research.1-70.v1.

Klocke, C., Allen, J.L., Sobolewski, M., Blum, J.L., Zelikoff, J.T., Cory-Slechta, D.A., 2018. Exposure to fine and ultrafine particulate matter during gestation alters postnatal oligodendrocyte maturation, proliferation capacity, and myelination. Neurotoxicology 65, 196–206. https://doi.org/10.1016/j.neuro.2017.10.004.

Klocke, C., Allen, J.L., Sobolewski, M., Mayer-Proschel, M., Blum, J.L., Lauterstein, D., Zelikoff, J.T., Cory-Slechta, D.A., 2017. Neuropathological consequences of gestational exposure to concentrated ambient fine and ultrafine particles in the mouse.

Toxicol. Sci. 156, 492–508. https://doi.org/10.1093/toxsci/kfx010.
Levesque, S., Surace, M.J., McDonald, J., Block, M.L., 2011. Air pollution & the brain: Subchronic diesel exhaust exposure causes neuroinflammation and elevates early markers of neurodegenerative disease. J. Neuroinflammation 8, 105. https://doi.org/10.1186/1742-2094-8-105.
Li, D., Morishita, M., Wagner, J.G., Fatouraie, M., Wooldridge, M., Eagle, W.E., Barres, J., Carlander, U., Emond, C., Jolliet, O., 2016. In vivo biodistribution and physiologically based pharmacokinetic modeling of inhaled fresh and aged cerium oxide nanoparticles in rats. Part. Fibre. Toxicol. 13, 45. https://doi.org/10.1186/s12989-016-0156-2.
Lison, D., Lardot, C., Huaux, F., Zanetti, G., Fubini, B., 1997. Influence of particle surface area on the toxicity of insoluble manganese dioxide dusts. Arch. Toxicol. 71, 725–729. https://doi.org/10.1007/s002040050453.
Liu, C., Fonken, L.K., Wang, A., Maiseyeu, A., Bai, Y., Wang, T.Y., Maurya, S., Ko, Y.A., Periasamy, M., Dvonch, T., Morishita, M., Brook, R.D., Harkema, J., Ying, Z., Mukherjee, B., Sun, Q., Nelson, R.J., Rajagopalan, S., 2014. Central IKKbeta inhibition prevents air pollution mediated peripheral inflammation and exaggeration of type II diabetes. Part. Fibre. Toxicol. 11, 53. https://doi.org/10.1186/s12989-014-0053-5.
Maher, B.A., Ahmed, I.A., Karloukovski, V., MacLaren, D.A., Foulds, P.G., Allsop, D., Mann, D.M., Torres-Jardon, R., Calderon-Garcidueñas, L., 2016. Magnetite pollution nanoparticles in the human brain. Proc. Natl. Acad. Sci. USA 113, 10797–10801. https://doi.org/10.1073/pnas.1605941113.
McCallister, M.M., Maguire, M., Ramesh, A., Aimin, Q., Liu, S., Khoshbouei, H., Aschner, M., Ebner, F.F., Hood, D.B., 2008. Prenatal exposure to benzo(a)pyrene impairs later-life cortical neuronal function. Neurotoxicology 29, 846–854. https://doi.org/10.1016/j.neuro.2008.07.008.
Misra, C., Kim, S., Shen, S., Sioutas, C., 2002. A high flow rate, very low pressure drop impactor for inertial separation of ultrafine from accumulation mode particles. J. Aerosol. Sci. 33, 735–752. https://doi.org/10.1016/S0021-8502(01)00210-5.
Morgan, T.E., Davis, D.A., Iwata, N., Tanner, J.A., Snyder, D., Ning, Z., Kam, W., Hsu, Y.T., Winkler, J.W., Chen, J.C., Petasis, N.A., Baudry, M., Sioutas, C., Finch, C.E., 2011. Glutamatergic neurons in rodent models respond to nanoscale particulate urban air pollutants in vivo and in vitro. Environ. Health. Perspect. 119, 1003–1009. https://doi.org/10.1289/ehp.1002973.
Mumaw, C.L., Levesque, S., McGraw, C., Robertson, S., Lucas, S., Stafflinger, J.E., Campen, M.J., Hall, P., Norenberg, J.P., Anderson, T., Lund, A.K., McDonald, J.D., Ottens, A.K., Block, M.L., 2016. Microglial priming through the lung-brain axis: the role of air pollution-induced circulating factors. FASEB. J. 30, 1880–1891. https://doi.org/10.1096/fj.201500047.
Oberdorster, G., Oberdorster, E., Oberdorster, J., 2005. Nanotoxicology: an emerging discipline evolving from studies of ultrafine particles. Environ. Health. Perspect. 113, 823–839. https://doi.org/10.1289/ehp.7339.
Paul, K.C., Haan, M., Mayeda, E.R., Ritz, B.R., 2019. Ambient Air Pollution, Noise, and Late-Life Cognitive Decline and Dementia Risk. Annu. Rev. Public. Health 40, 203–220. https://doi.org/10.1146/annurev-publhealth-040218-044058.
Peters, R., Ee, N., Peters, J., Booth, A., Mudway, I., Anstey, K.J., 2019. Air pollution and dementia: a systematic review. J. Alzheimers. Dis. 70, S145–S163. https://doi.org/10.3233/JAD-180631.
Peterson, B.S., Rauh, V.A., Bansal, R., Hao, X., Toth, Z., Nati, G., Walsh, K., Miller, R.L., Arias, F., Semanek, D., Perera, F., 2015. Effects of prenatal exposure to air pollutants (polycyclic aromatic hydrocarbons) on the development of brain white matter, cognition, and behavior in later childhood. JAMA Psychiatry 72, 531–540. https://doi.org/10.1001/jamapsychiatry.2015.57.
Pfalzgraff, A., Correa, W., Heinbockel, L., Schromm, A.B., Lubow, C., Gisch, N., Martinez-de-Tejada, G., Brandenburg, K., Weindl, G., 2019. LPS-neutralizing peptides reduce outer membrane vesicle-induced inflammatory responses. Biochim. Biophys. Acta. Mol. Cell. Biol. Lipids 1864, 1503–1513. https://doi.org/10.1016/j.bbalip.2019.05.018.
Pirhadi, M., Mousavi, A., Taghvaee, S., Sowlat, M.H., Sioutas, C., 2019. An aerosol concentrator/diffusion battery tandem to concentrate and separate ambient accumulation mode particles for evaluating their toxicological properties. Atmos. Environ. 213, 81–89. https://doi.org/10.1016/j.atmosenv.2019.05.058.
Premasekharan, G., Nguyen, K., Contreras, J., Ramon, V., Leppert, V.J., Forman, H.J., 2011. Iron-mediated lipid peroxidation and lipid raft disruption in low-dose silica-induced macrophage cytokine production. Free. Radic. Biol. Med. 51, 1184–1194. https://doi.org/10.1016/j.freeradbiomed.2011.06.018.
Reich, J., Tamura, H., Nagaoka, I., Motschmann, H., 2018. Investigation of the kinetics and mechanism of low endotoxin recovery in a matrix for biopharmaceutical drug products. Biologicals 53, 1–9. https://doi.org/10.1016/j.biologicals.2018.04.001.
Sang, N., Yun, Y., Li, H., Hou, L., Han, M., Li, G., 2010. SO2 inhalation contributes to the development and progression of ischemic stroke in the brain. Toxicol. Sci. 114, 226–236. https://doi.org/10.1093/toxsci/kfq010.
Saunders, C.R., Das, S.K., Ramesh, A., Shockley, D.C., Mukherjee, S., 2006. Benzo(a) pyrene-induced acute neurotoxicity in the F-344 rat: role of oxidative stress. J. Appl. Toxicol. 26, 427–438. https://doi.org/10.1002/jat.1157.
Sheesley, R.J., Schauer, J.J., Chowdhury, Z., Cass, G.R., Simoneit, B.R., 2003. Characterization of organic aerosols emitted from the combustion of biomass indigenous to South Asia. J. Geophys. Res. Atmosph. 108. https://doi.org/10.1029/2002JD002981.
Stepien, G., Moros, M., Perez-Hernandez, M., Monge, M., Gutierrez, L., Fratila, R.M., Las Heras, M., Menao Guillen, S., Puente Lanzarote, J.J., Solans, C., Pardo, J., de la Fuente, J.M., 2018. Effect of surface chemistry and associated protein corona on the long-term biodegradation of iron oxide nanoparticles in vivo. ACS. Appl. Mater. Interfaces 10, 4548–4560. https://doi.org/10.1021/acsami.7b18648.
Stone, E.A., Hedman, C.J., Sheesley, R.J., Shafer, M.M., Schauer, J.J., 2009. Investigating the chemical nature of humic-like substances (HULIS) in North American atmospheric aerosols by liquid chromatography tandem mass spectrometry. Atmos. Environ. 43, 4205–4213. https://doi.org/10.1016/j.atmosenv.2009.05.030.
Taghvaee, S., Mousavi, A., Sowlat, M.H., Sioutas, C., 2019. Development of a novel aerosol generation system for conducting inhalation exposures to ambient particulate matter (PM). Sci. Total. Environ. 665, 1035–1045. https://doi.org/10.1016/j.scitotenv.2019.02.214.
Tyler, C.R., Noor, S., Young, T.L., Rivero, V., Sanchez, B., Lucas, S., Caldwell, K.K., Milligan, E.D., Campen, M.J., 2018. Aging exacerbates neuroinflammatory outcomes induced by acute ozone exposure. Toxicol. Sci. 163, 123–139. https://doi.org/10.1093/toxsci/kfy014.
Valdez, M.C., Freeborn, D., Valdez, J.M., Johnstone, A.F.M., Snow, S.J., Tennant, A.H., Kodavanti, U.P., Kodavanti, P.R.S., 2019. Mitochondrial bioenergetics in brain following ozone exposure in rats maintained on coconut, fish and olive oil-rich diets. Int. J. Mol. Sci. 20, 6303. https://doi.org/10.3390/ijms20246303.
Volk, H.E., Hertz-Picciotto, I., Delwiche, L., Lurmann, F., McConnell, R., 2011. Residential proximity to freeways and autism in the CHARGE study. Environ. Health. Perspect. 119, 873–877. https://doi.org/10.1289/ehp.1002835.
Wang, D.B., Pakbin, P., Saffari, A., Shafer, M.M., Schauer, J.J., Sioutas, C., 2013. Development and evaluation of a high-volume aerosol-into-liquid collector for fine and ultrafine particulate matter. Aerosol. Sci. Tech. 47, 1226–1238. https://doi.org/10.1080/02786826.2013.830693.
Ward, E.C., Murray, M.J., Lauer, L.D., House, R.V., Irons, R., Dean, J.H., 1984. Immunosuppression following 7,12-dimethylbenz[a]anthracene exposure in B6C3F1 mice. I. Effects on humoral immunity and host resistance. Toxicol. Appl. Pharmacol. 75, 299–308. https://doi.org/10.1016/0041-008x(84)90212-6.
Woodward, N.C., Crow, A.L., Zhang, Y., Epstein, S., Hartiala, J., Johnson, R., Kocalis, H., Saffari, A., Sankaranarayanan, I., Akbari, O., Ramanathan, G., Araujo, J.A., Finch, C.E., Bouret, S.G., Sioutas, C., Morgan, T.E., Allayee, H., 2019. Exposure to Nanoscale Particulate Matter from Gestation to Adulthood Impairs Metabolic Homeostasis in Mice. Sci. Rep. 9, 1816. https://doi.org/10.1038/s41598-018-37704-2.
Woodward, N.C., Haghani, A., Johnson, R.G., Hsu, T.M., Saffari, A., Sioutas, C., Kanoski, S.E., Finch, C.E., Morgan, T.E., 2018. Prenatal and early life exposure to air pollution induced hippocampal vascular leakage and impaired neurogenesis in association with behavioral deficits. Transl. Psychiatry 8, 261. https://doi.org/10.1038/s41398-018-0317-1.
Woodward, N.C., Levine, M.C., Haghani, A., Shirmohammadi, F., Saffari, A., Sioutas, C., Morgan, T.E., Finch, C.E., 2017a. Toll-like receptor 4 in glial inflammatory responses to air pollution in vitro and in vivo. J. Neuroinflammation 14, 84. https://doi.org/10.1186/s12974-017-0858-x.
Woodward, N.C., Pakbin, P., Saffari, A., Shirmohammadi, F., Haghani, A., Sioutas, C., Cacciottolo, M., Morgan, T.E., Finch, C.E., 2017b. Traffic-related air pollution impact on mouse brain accelerates myelin and neuritic aging changes with specificity for CA1 neurons. Neurobiol. Aging 53, 48–58. https://doi.org/10.1016/j.neurobiolaging.2017.01.007.
Wormley, D.D., Chirwa, S., Nayyar, T., Wu, J., Johnson, S., Brown, L.A., Harris, E., Hood, D.B., 2004. Inhaled benzo(a)pyrene impairs long-term potentiation in the F1 generation rat dentate gyrus. Cell. Mol. Biol. (Noisy-le-grand) 50, 715–721.
Yan, W., Ku, T., Yue, H., Li, G., Sang, N., 2016. NO2 inhalation causes tauopathy by disturbing the insulin signaling pathway. Chemosphere 165, 248–256. https://doi.org/10.1016/j.chemosphere.2016.09.063.
Yang, T.T., Sinai, P., Kitts, P.A., Kain, S.R., 1997. Quantification of gene expression with a secreted alkaline phosphatase reporter system. Biotechniques 23, 1110–1114. https://doi.org/10.2144/97236pf01.
Zhang, H., Haghani, A., Mousavi, A.H., Cacciottolo, M., D'Agostino, C., Safi, N., Sowlat, M.H., Sioutas, C., Morgan, T.E., Finch, C.E., Forman, H.J., 2019. Cell-based assays that predict in vivo neurotoxicity of urban ambient nano-sized particulate matter. Free. Radic. Biol. Med 145, 33–41. https://doi.org/10.1016/j.freeradbiomed.2019.09.016.
Zhang, M., Liu, W., Zhou, Y., Li, Y., Qin, Y., Xu, Y., 2018. Neurodevelopmental toxicity induced by maternal PM2.5 exposure and protective effects of quercetin and Vitamin C. Chemosphere 213, 182–196. https://doi.org/10.1016/j.chemosphere.2018.09.009.
Zheng, X., Wang, X., Wang, T., Zhang, H., Wu, H., Zhang, C., Yu, L., Guan, Y., 2018. Gestational exposure to particulate matter 2.5 (PM2.5) leads to spatial memory dysfunction and neurodevelopmental impairment in hippocampus of mice offspring. Front. Neurosci. 12, 1000. https://doi.org/10.3389/fnins.2018.01000.